The effects on Trypanosoma cruzi of novel synthetic naphthoquinones are mediated by mitochondrial dysfunction

ARTICLE *in* FREE RADICAL BIOLOGY AND MEDICINE · JULY 2009

Impact Factor: 5.74 · DOI: 10.1016/j.freeradbiomed.2009.06.004 · Source: PubMed

7 AUTHORS, INCLUDING:

Renata L S Goncalves
Harvard University
25 PUBLICATIONS **296** CITATIONS
SEE PROFILE

Raphael S F Silva
Instituto Federal de Educação, Ciência e Te…
24 PUBLICATIONS **282** CITATIONS
SEE PROFILE

Marcus Oliveira
Federal University of Rio de Janeiro
57 PUBLICATIONS **1,641** CITATIONS
SEE PROFILE

Solange Castro
Fundação Oswaldo Cruz
118 PUBLICATIONS **4,298** CITATIONS
SEE PROFILE

J Bioenerg Biomembr (2011) 43:651–661
DOI 10.1007/s10863-011-9398-8

A comparative assessment of mitochondrial function in epimastigotes and bloodstream trypomastigotes of *Trypanosoma cruzi*

Renata L. S. Gonçalves · Rubem F. S. Menna Barreto · Carla R. Polycarpo · Fernanda R. Gadelha · Solange L. Castro · Marcus F. Oliveira

Received: 9 August 2011 / Accepted: 28 September 2011 / Published online: 12 November 2011

Abstract *Trypanosoma cruzi* is a hemoflagellate protozoan that causes Chagas' disease. The life cycle of *T. cruzi* is complex and involves different evolutive forms that have to encounter different environmental conditions provided by the host. Herein, we performed a functional assessment of mitochondrial metabolism in the following two distinct evolutive forms of *T. cruzi*: the insect stage epimastigote and the freshly isolated bloodstream trypomastigote. We observed that in comparison to epimastigotes, bloodstream trypomastigotes facilitate the entry of electrons into the electron transport chain by increasing complex II-III activity. Interestingly, cytochrome *c* oxidase (CCO) activity and the expression of CCO subunit IV were reduced in bloodstream forms, creating an "electron bottleneck" that favored an increase in electron leakage and H_2O_2 formation. We propose that the oxidative preconditioning provided by this mechanism confers protection to bloodstream trypomastigotes against the host immune system. In this scenario, mitochondrial remodeling during the *T. cruzi* life cycle may represent a key metabolic adaptation for parasite survival in different hosts.

Keywords Energy metabolism · Reactive oxygen species · Hormesis · Differentiation

This work is dedicated to the memory of the honorable Brazilian scientist, teacher and human being Dr. Henrique Leonel Lenzi (1943–2011).

R. L. S. Gonçalves · M. F. Oliveira (✉)
Laboratório de Bioquímica de Resposta ao Estresse,
Programa de Biologia Molecular e Biotecnologia,
Instituto de Bioquímica Médica,
Universidade Federal do Rio de Janeiro,
Rio de Janeiro, RJ, Brazil
e-mail: maroli@bioqmed.ufrj.br

R. L. S. Gonçalves · M. F. Oliveira
Laboratório de Inflamação e Metabolismo,
Instituto Nacional de Ciência e Tecnologia de
Biologia Estrutural e Bioimagem (INBEB),
Universidade Federal do Rio de Janeiro,
Rio de Janeiro, RJ, Brazil

R. F. S. M. Barreto · S. L. Castro
Laboratório de Biologia Celular, Instituto Oswaldo Cruz,
FIOCRUZ,
Rio de Janeiro, RJ, Brazil

C. R. Polycarpo
Laboratório de Biologia Molecular,
Programa de Biologia Molecular e Biotecnologia,
Instituto de Bioquímica Médica,
Universidade Federal do Rio de Janeiro,
Rio de Janeiro, RJ, Brazil

F. R. Gadelha
Departamento de Bioquímica, Instituto de Biologia,
Universidade Estadual de Campinas,
Campinas, SP, Brazil

Introduction

Chagas' disease, once thought to be an endemic illness in Latin America, affects approximately 12–14 million people (Dias 2007) and has spread to other regions, such as North America, Europe and Japan (Tanowitz et al. 2011). The life cycle of the etiological agent *Trypanosoma cruzi* is complex, involving four different evolutive forms that have to develop inside hematophagous triatomine insect vectors and mammalian hosts. Inside the vertebrate host, *T. cruzi* transforms into a bloodstream non-dividing form referred to as a trypomastigote, which subsequently transforms into an intracellular dividing form, the amastigote. Inside the insect host, *T. cruzi* develops into either proliferative or non-

proliferative infective forms known as epimastigotes and metacyclic trypomastigotes, respectively. Thus, the adaptation of different parasite evolutive forms to changes in environmental and physico-chemical conditions is an important survival mechanism.

The members of the *Trypanosomatidae* family exhibit several distinct features, such as the presence of glycosomes, which are peroxisome-like organelles that compartmentalize the first reactions of glycolysis (Michels et al. 2006). These parasites possess a single mitochondrion that remains morphologically similar throughout their life cycle (de Meirelles and De Souza 1982). Regarding energy metabolism, the life stages of *T. cruzi* and *Leishmania* exhibit a comparatively more complex metabolic capacity than other trypanosomatids because they are able to metabolize glucose and amino acids (Rogerson and Gutteridge 1980). Although *T. cruzi* metabolism changes considerably over its life cycle, the different stages have functional tricarboxylic acid cycles (Adroher et al. 1988; Rogerson and Gutteridge 1980) and oxidative phosphorylation machinery (Tielens and Van Hellemond 2009). *T. cruzi* experiences differences in glucose availability being the vertebrate blood rich in glucose (Lehane 2005), whereas the insect digestive tract has limited amounts of free glucose (Billingsley 1988). The vertebrate form trypomastigotes exhibits the highest glucose transport activity (Silber et al. 2009), and its transition to amastigotes is accompanied by a shift from a carbohydrate- to a lipid-based energy metabolism (Atwood et al. 2005).

Mitochondria are organelles that are implicated not only in aerobic ATP synthesis via oxidative phosphorylation but are also involved in the cellular redox balance, representing one of the major sources of reactive oxygen species (ROS) in the cell. During mitochondrial respiration, a small portion of oxygen is partially reduced to superoxide ($O_2^{\bullet-}$) radicals, which are then dismutated to hydrogen peroxide (H_2O_2) by superoxide dismutase (SOD) (Boveris and Chance 1973; Brookes et al. 2002) or spontaneous reduction. The redox state of the mitochondrial electron transport chain (ETC) is crucial for ROS generation (Nicholls and Ferguson 2002). Under a higher mitochondrial membrane potential ($\Delta\Psi m$), the half-life of the reduced ETC components increases, favoring the leakage of electrons (Kowaltowski et al. 2009; Korshunov et al. 1997). Controlled levels of ROS are important for signaling and adaptation to a number of different insults (Pan et al. 2011). Mitochondrial, microsomal and cytosolic enzymes contribute to H_2O_2 generation at fairly high rates in *T. cruzi* epimastigotes (Boveris and Stoppani 1977; Carranza et al. 2009). Interestingly, parasites with increased antioxidant defenses are more resistant to redox insults and are more virulent, suggesting a relationship between redox balance and infectivity (Piacenza et al. 2009). Finally, the transformation of epimastigotes to infective metacyclic trypomastigotes entails an increase in some of the parasite antioxidant defenses, which can be seen as important mechanisms to circumvent the redox challenge mediated by the host immune system (Atwood et al. 2005).

Recent findings demonstrate that complex I of the respiratory chain has limited functions in *T. cruzi* metabolism (Carranza et al. 2009; Silva et al. 2011). Additionally, succinate has been shown to be the main substrate that supports oxygen consumption in epimastigotes (Denicola-Seoane et al. 1992; Vercesi et al. 1991). The levels of cytochromes *b* and *a* are significantly lower in *T. cruzi* epimastigotes in comparison with those in mammalian cells (Cazzulo 1994). Cytochrome *a* is part of complex IV, which is the rate limiting step in mitochondrial respiration (Poyton and McEwen 1996; Villani et al. 1998; Villani and Attardi 2000). The inhibition of complex IV activity increases the reduction state of the upstream ETC components, impairing the respiratory rates and oxidative phosphorylation, thereby favoring ROS formation (Ferguson et al. 2005; Zuckerbraun et al. 2007). Another peculiarity of the trypanosomatid respiratory chain is the presence of a cyanide-insensitive salicylhydroxamic acid (SHAM)-sensitive terminal oxidase (alternative oxidase), which is important for regenerating glycosomal NADH (Chaudhuri et al. 2006).

Using an enhanced method to culture trypomastigotes, Docampo et al. demonstrated select features of the *T. cruzi* mitochondrion (Docampo et al. 1993; Docampo 1993). Aside from these previous reports, the efforts to characterize mitochondrial physiology in different *T. cruzi* forms have been hampered by the difficulties in obtaining freshly isolated bloodstream trypomastigotes. Therefore, we aimed to compare the mitochondrial function between freshly isolated bloodstream *T. cruzi* trypomastigotes with epimastigotes. Because *T. cruzi* experiences strikingly distinct environmental challenges in hosts, we hypothesized that mitochondrion functional plasticity would be central in enabling the parasite to adapt to such variations. We demonstrated that the mitochondrion of *T. cruzi* bloodstream trypomastigotes exhibits lower oxygen consumption rates and increased H_2O_2 production in comparison to those of the insect stage epimastigotes. The increased electron leakage observed in bloodstream trypomastigotes could be a consequence of the increased activity of complex II–III and the reduced activity of complex IV. We propose that this is a redox-mediated preconditioning that would confer some protection to bloodstream trypomastigotes against an oxidative challenge induced by host immune system activation.

Material and methods

Parasites All experiments were performed with the *T. cruzi* Y strain. Epimastigotes were maintained axenically at 28 °C

in a liver infusion and tryptose (LIT) medium supplemented with 10% fetal bovine serum (FBS) (Cultilab, Campinas, Brazil). The medium was changed weekly, and epimastigotes were harvested during the exponential growth phase (5-day old cultures). Bloodstream trypomastigotes were isolated from the blood of albino Swiss mice 7 days after intraperitoneal injection with 5×10^5 parasites. Citrated blood was collected by heart puncture. Red and white blood cells were removed by differential centrifugation (500 x *g* for 30 min at 4 °C), and the supernatant was collected to obtain the purified parasites. To improve the yield of parasites, the pellet was resuspended in Dulbecco's modified Eagle's medium (DMES, Sigma-Aldrich, St. Louis, MO, USA) supplemented with 10% FBS and re-centrifuged at 500 x *g* for 15 min. This step was repeated two times, the supernatants were centrifuged (1,500 x *g* for 15 min) and bloodstream trypomastigote pellets were resuspended in 3–5 mL of DMES+10% FBS. Finally, the parasites were washed with phosphate buffered saline (PBS) and kept on ice until use. The yield of this procedure was approximately 2.5×10^7 parasites/mouse. The protein concentration in both parasite forms was determined by the Lowry method (Lowry et al. 1951) using bovine serum albumin as the standard.

Susceptibility of T. cruzi to different compounds Bloodstream trypomastigotes and epimastigotes were respectively resuspended in DMES and LIT media supplemented with 10% FBS. An aliquot of 100 μL (10^6 parasites) was added to the same volume of H_2O_2, antimycin A (AA) or iodoacetamide (IAA) previously prepared at twice the desired final concentration in 96-well microplates and incubated at 37 °C (trypomastigotes) or 28 °C (epimastigotes) for 2 h. Cell counts were performed on a Neubauer chamber, and the activity of the compounds upon parasite survival was expressed as LD_{50}, corresponding to the concentration that leads to the lysis of 50% parasites.

Mitochondrial membrane potential Parasite mitochondrial membrane potential ($\Delta\Psi_m$) was evaluated fluorimetrically by the following two different approaches: i) TMRE probe on intact cells; ii) safranine O in digitonin-permeabilized cells. For the TMRE analysis, epimastigotes and bloodstream trypomastigotes were incubated with 50 nM of the probe for 20 min. TMRE-positive parasites were analyzed using a FACSCalibur flow cytometer (Becton Dickinson, Franklin Lakes, NJ, USA) equipped with Cell Quest software (Joseph Trotter, Scripps Research Institute, La Jolla, CA, USA). The specificity of TMRE staining was evaluated by inducing mitochondrial uncoupling after the addition of 1 μM FCCP. A total of 10,000 events were acquired in the region previously established to correspond to parasites. Safranin O fluorescence was measured with a spectrofluorometer (excitation and emission at 495 and 586 nm wavelengths, respectively) (Varian, Cary Eclipse Model, Oberkochen, Germany). A sample of 5×10^7 parasites was added to 2 mL of respiration buffer containing 125 mM sucrose, 65 mM KCl, 2 mM KH_2PO_4, 0.5 mM $MgCl_2$, 10 mM HEPES-KOH (pH 7.2), 1 mg/mL fatty acid free bovine serum albumin (FAF-BSA), and 1 mM EGTA (Vercesi et al. 1991 with minor modifications). Succinate (5 mM) was added to energize the mitochondria. The digitonin concentration was titrated based on the loss of fluorescence of safranin O. Optimal digitonin concentrations for each parasite form, 15 μM for epimastigotes and 7.5 μM for the trypomastigotes, were set based on the maintenance of the $\Delta\Psi_m$ for at least 30 min. The $\Delta\Psi_m$ collapsed after adding 1.25 μg/mL AA.

ETC complex activities Mitochondrial ETC complex activities were measured in triplicate at room temperature in a total reaction volume of 1 mL using a spectrophotometer (UV 2550 Shimadzu Co., Shimadzu, Japan) as previously described (Ferguson et al. 2005). The AA-sensitive succinate:cytochrome c oxidoreductase activity (complex II–III) was measured by the increase in the absorbance at 550 nm due to the reduction of ferricytochrome c (ε=19 mM^{-1} cm^{-1}) (Chance and Williams 1955). The reaction mixture consisted of 100 mM potassium phosphate buffer (pH 7.4), 50 μM horse heart cytochrome *c*, 5 mM succinate and 1 mM KCN. KCN-sensitive cytochrome *c* oxidase (complex IV) activity was measured based on the decrease in absorbance due to the oxidation of ferrocytochrome *c* at 550 nm (ε=19 mM^{-1} cm^{-1}). The reaction mixture consisted of 100 mM potassium phosphate buffer (pH 7.4) and 50 μM sodium dithionite-reduced cytochrome *c*. Decreases in absorbance were monitored after the addition of frozen-thawed parasite homogenates (70 μg of protein).

F_1F_o ATP synthase functional content To assess the functional content of F_1F_o ATP synthase, basal respiratory rates of epimastigotes and bloodstream trypomastigotes kept in respiration buffer were titrated with oligomycin (0.1 μg/mL) until they reached a state-4 like respiratory rates, meaning that any further addition of oligomycin was unable to decrease the oxygen consumption rates. The basal respiratory rates were plotted against the doses of oligomycin, and the functional content was calculated as described in Japiassu et al. (2011).

Oxygen consumption rates O_2 consumption rates of epimastigotes or trypomastigotes (5×10^7 parasites/chamber) were evaluated by high-resolution respirometry (Oxygraph-2 K; OROBOROS Instruments, Innsbruck, Austria) under continuous stirring. The temperature was maintained at 28 °C

for experiments with epimastigotes and at 37 °C for trypomastigotes. Both reactions were performed in 2 mL of respiration buffer. Oxygen concentration and flux were recorded using DatLab software (Oxygraph-2 K; ORO-BOROS Instruments, Innsbruck, Austria). Digitonin (15 μM for epimastigotes and 7.5 μM for trypomastigotes) was added to permeabilize the parasites. Subsequently, 5 mM succinate and 200 μM ADP were added to stimulate state 3 mitochondrial oxygen consumption. State 4-like respiration was induced with the addition of 2.5 μg/mL oligomycin as described by Vercesi et al. (1991). Uncoupled respiration was stimulated after the addition of up to 3 μM FCCP, resulting in increased oxygen consumption. Mitochondrial respiration was inhibited by the addition of 1.25 μg/mL of AA to reach residual oxygen consumption (ROX).

Mitochondrial H_2O_2 release H_2O_2 release was measured using the Amplex Red probe (Molecular Probes, Carlsbad, CA, USA) and horseradish peroxidase (HRP; Sigma-Aldrich, St. Louis, MO, USA) (Votyakova and Reynolds 2004). Epimastigotes or trypomastigotes (5 x 10^7/chamber) were incubated in the respiration buffer described above containing 2.5 μM Amplex Red reagent and 3 U/mL HRP. Parasites were permeabilized with the same digitonin concentrations set for the respirometry assays. Mitochondrial metabolic states were measured following the same protocol employed for the oxygen consumption measurements. Amplex Red fluorescence was monitored at excitation and emission wavelengths at 530 nm (slit 5 nm) and 590 nm (slit 5 nm), respectively, in a Varian spectrofluorometer (Cary Eclipse Model, Oberkochen, Germany). A calibration curve was obtained using H_2O_2 as a standard (Menna-Barreto et al. 2009).

Mitochondrial free radical leak Both oxygen consumption rates and H_2O_2 release were measured in the same media, as well as at the same temperature and substrate concentration. The free radical leak was considered as the percentage of electrons out of sequence that reduced oxygen to superoxide (which is further dismutated to H_2O_2) instead of reaching complex IV to reduce oxygen to water. The rates of H_2O_2 release were divided by twice the rate of oxygen consumed in the same mitochondrial metabolic state; percentages of these values were obtained by multiplication by 100 (Herrero and Barja 1997).

Real time PCR Parasite total RNA was extracted using TRIzol reagent according to the manufacturer's instructions. Up to 1 μg of RNA was treated with DNAse I (Fermentas, Thermo Fisher Scientific Inc., Canada) to avoid genomic DNA contamination. The complementary DNA (cDNA) was synthesized using the High-capacity Reverse Transcriptase Polymerase Chain Reaction (RT-PCR) kit (Applied Biosystems, USA). Quantitative PCR was performed in a StepOnePlus Real time PCR machine (Applied Biosystems, USA) using the Power SYBR-Green PCR Master Mix (Applied Biosystems, USA). The $2^{-\Delta\Delta Ct}$ method was used to analyze the relative changes in gene expression levels (Livak and Schmittgen 2001). Alpha tubulin (accession number: Tc00.1047053411235.9) was used as an endogenous control. The PCR program consisted of a heating at 95 °C for 10 min followed by 40 cycles at 95 °C for 15 s, 60 °C for 1 min and a melting curve. The oligonucleotides were designed using primer3 software (Rozen and Skaletsky 2000) after the identification of *T. cruzi* orthologs for succinate dehydrogenase (accession number: Tc00.1047053505843.24), cytochrome *b* (accession number: Tc00.1047053509395.100) and cytochrome *c* oxidase, and subunit IV (accession number: Tc00.1047053510889.50). The following primer sequences were used: L- GGCTTTGGAAACAACCCATA and R-TCAATCAACCAGCGATACGA for succinate dehydrogenase; L- GGTCACAGTGAACAGGCAAA and R-CCCCAACGAAAGAAATACCA for cytochrome *b* and cytochrome *c* oxidase; and L-CTACGTGAAAAGACGCG TTG and R- GCATACTCCCGCTCAACATT for subunit IV.

Statistical analyses Comparisons between groups were performed by one-way ANOVA followed by Tukey's test for pairwise comparison. When appropriate, unpaired Student's *t*-tests were employed. Statistical analysis was performed using GraphPad Prism version 4.00 for Windows (GraphPad Software, San Diego, USA). Significance levels were indicated by $P \leq 0.05$. All experiments were performed with at least three independent sample groups.

Results

Epimastigotes and bloodstream trypomastigotes exhibit different susceptibilities to energy and redox metabolism modulators

Our first goal was to determine the susceptibility of *T. cruzi* epimastigotes and bloodstream trypomastigotes to iodoacetamide (IAA) and antimycin a (AA), which are classical inhibitors of glyceraldehyde-3-phosphate dehydrogenase (glycolysis) and mitochondrial ETC complex III, respectively. Table 1 shows that bloodstream trypomastigotes are more sensitive to the inhibition of glycolysis than epimastigotes due to their significantly lower LD_{50} value for IAA (171.2±38.7 μM vs. 1818.4±258.4 μM, $p<0.004$). However, bloodstream trypomastigotes were more resistant to ETC inhibition than epimastigotes, exhibiting a higher LD_{50} value for AA (193.4±13.3 μM vs. 40.6±5.9 μM, $p<0.02$). Interestingly, the bloodstream forms were also more

Table 1 The effect of iodoacetamide, Antimycin A and H_2O_2 on *T. cruzi* epimastigotes and trypomastigotes survival[a]

	Epimastogotes	Trypomastigotes
Iodoacetamide	1818.4±258.4 (n=6)	171.2**±38.7 (n=6)
Antimcin A	40.6±5.9 (n=4)	193.4*±13.3 (n=4)
H_2O_2	694.2±33.1 (n=4)	14.30.5*±140.3 (n=4)

[a] Values were expressed as mean ± SD of LD_{50} of each compound (μM) after 2 h incubation. Data was collected from at least three independent experiments. *, $p<0.02$; **, $p<0.004$ Student's*t*-test statistical analyses for comparisons between trypamastigotes and epimastigotes

resistant to oxidative stress, as revealed by higher LD_{50} values for H_2O_2 (1430.5±140.3 μM vs. 694.2±33.1 μM, $p<0.02$). These results indicate that *T. cruzi* bloodstream trypomastigotes rely more on glycolysis than oxidative phosphorylation to meet their energy demand, and are more resistant to redox challenges than epimastigotes.

Bloodstream trypomastigotes exhibit lower mitochondrial membrane potential than epimastigotes

Based on the results of Table 1, the next set of experiments was designed to perform a functional assessment of the mitochondrion of both parasite forms. Our first task was to evaluate the mitochondrial membrane potential ($\Delta\Psi_m$) on intact bloodstream trypomastigotes and epimastigotes by staining parasites with the fluorescent probe TMRE, which accumulates in energized mitochondria. Flow cytometry analysis showed that epimastigotes (Fig. 1a, in black) exhibited higher TMRE fluorescence than bloodstream trypomastigotes (in gray). In order to validate the measurements, both *T. cruzi* forms were incubated with the proton ionophore FCCP, which collapses the $\Delta\Psi_m$, decreasing TMRE fluorescence intensities. As expected, the white peaks of Fig. 1a show that FCCP incubation reduced TMRE fluorescence in both parasite forms. TMRE fluorescence revealed that bloodstream forms have lower $\Delta\Psi_m$ ($p<0.05$) than those of epimastigotes (Fig. 1b). The prevalence of TMRE fluorescence was drastically reduced ($p<0.001$) after FCCP incubation regardless of the parasite form (Fig. 1c). Figure 1a–c indicate that the assessment of the $\Delta\Psi_m$ on intact parasite forms using TMRE staining was successful. We also evaluated the succinate-induced $\Delta\Psi_m$ on digitonin-permeabilized epimastigotes and bloodstream trypomastigotes using the Safranine O method. The permeabilization efficiency was monitored by the decrease of Safranine O fluorescence in the presence of 5 mM succinate. Optimal digitonin concentrations of 7.5 μM for bloodstream trypomastigotes and 15 μM for epimastigotes were sufficient to maintain a stable $\Delta\Psi_m$ for at least 30 min (data not shown). These digitonin concentrations were used in all cell-permeabilized experiments. Figure 1d shows that after digitonin permeabilization, both parasite forms generated a $\Delta\Psi_m$ that was more pronounced in insect stage epimastigotes than in bloodstream trypomastigotes. As expected, the AA addition caused a collapse of the $\Delta\Psi_m$ in both parasite forms. The results presented in Fig. 1 demonstrate that bloodstream trypomastigotes had a lower $\Delta\Psi_m$ compared to epimastigotes (Fig. 1d).

Bloodstream trypomastigotes exhibit lower respiratory rates specifically at mitochondrial metabolic states of high electron flux

The respiratory rates of parasites were assessed in digitonin-permeabilized epimastigotes and trypomastigotes

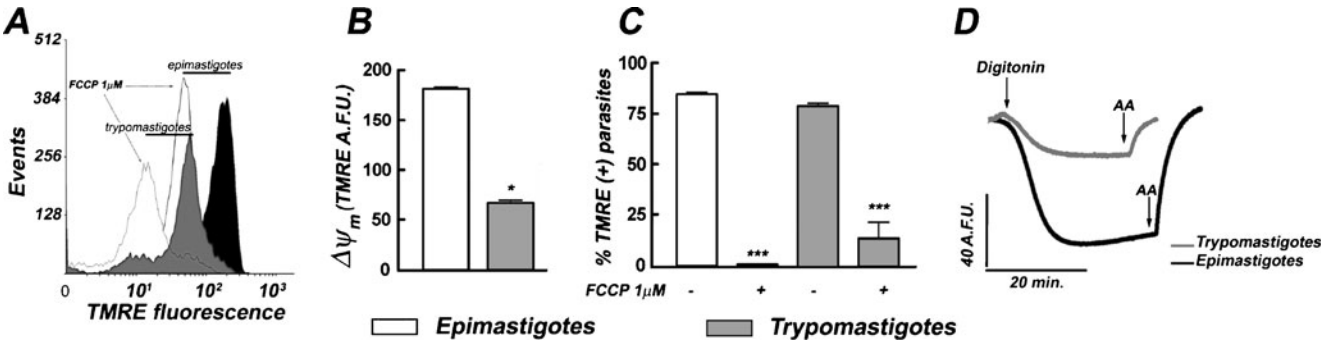

Fig. 1 Epimastigotes exhibit higher mitochondrial membrane potential ($\Delta\Psi_m$) than bloodstream trypomastigotes. (**a**) Representative flow cytometry histograms of TMRE fluorescence from epimastigotes (*black*) and bloodstream trypomastigotes (*gray*). The effect of 1 μM of the proton ionophore FCCP on the collapse of the $\Delta\Psi_m$ in both parasite forms is shown in white histograms. (**b**) TMRE fluorescence intensity was quantified for epimastigotes (*white bar*) and for bloodstream trypomastigotes (*gray bar*). (**c**) The percentage of TMRE-labeled epimastigotes (*white bars*) and bloodstream trypomastigotes (*gray bars*) and the effect of FCCP on the collapse of the $\Delta\Psi_m$. (**d**) Digitonin-permeabilized parasites were loaded with Safranine O to evaluate the membrane potential. Epimastigotes (*black line*) and bloodstream trypomastigotes (*gray line*) were permeabilized with 15 μM and 7.5 μM of the detergent, respectively. Antimycin A (1.25 μg/mL) was used to collapse the $\Delta\Psi$m. Data are expressed as the mean ± SEM. * $p<0.05$, the comparison of epimastigotes with bloodstream trypomastigotes; *** $p<0.001$, the comparison of control parasites with FCCP

using high-resolution respirometry with the same respiratory media as previously described (Vercesi et al. 1991; Carranza et al. 2009) in the presence of 5 mM succinate. Table 2 shows that ADP-induced state 3 respiration was significantly lower in bloodstream trypomastigotes than in epimastigotes (2.24±0.20 nmol O_2.min^{-1} mg^{-1} ptn vs. 3.5± 0.64 nmol O_2.min^{-1} mg^{-1} ptn, respectively, $p<0.05$). Induction of state 4 respiration by oligomycin strongly inhibited oxygen consumption rates down to similar levels in both parasite forms (bloodstream trypomastigotes: 1.14±0.18 nmol O_2.min^{-1} mg^{-1} ptn vs. epimastigotes: 1.29±0.16 nmol O_2.min^{-1} mg^{-1} ptn). The respiratory rates measured for epimastigotes in Table 2 agree with values obtained with strains CL Brener, Esmeraldo, and 115 epimastigote (Carranza et al. 2009). Uncoupled respiration in both parasite forms was achieved by titrating state 4 with the proton ionophore FCCP. As observed in state 3, uncoupled respiratory rates of trypomastigotes (1.9± 0.14 nmol O_2.min^{-1} mg^{-1} ptn) were significantly lower ($p<0.05$) than that in epimastigotes (3.51±0.44 nmol O_2.min^{-1} mg^{-1} ptn). Uncoupled respiratory rates were also indistinguishable from those in state 3. Residual oxygen consumption (ROX) was measured upon the addition of AA (1.25 μg/mL), which caused a reduction in oxygen consumption of 99.9% and 88% in epimastigotes and bloodstream trypomastigotes, respectively. Finally, the respiratory control ratio (RCR) in bloodstream trypomastigotes was determined to be 1.88±0.32, whereas epimastigotes exhibited a significantly higher value of 2.83±0.32 ($p<0.05$). The reduced RCR value in bloodstream trypomastigotes was essentially due to reduced uncoupled respiratory rates (Table 2).

Table 2 Oxygen consumption rates in digitonin-permeabilized *T. cruzi* in the presence of a FAD^+-linked substrate[a]

	Epimastigotes	Trypomastigotes
Mitochondrial metabolic states		
Succinate	1.89±0.38 (n=10)	1.73±0.33 (n=5)
ADP	3.5±0.64 (n=10)	2.24±0.29 (n=7)*
Oligo	1.29±0.16 (n=10)	1.14±0.18 (n=7)
FCCP	3.51±0.44 (n=10)	1.9±0.14 (n=7)*
ROX	0.15±0.09 (n=10)	0.23±0.06 (n=7)
RCR_{max}	2.839±0.32 (n=10)	1.887±0.32 (n=7)

[a] Values are expressed as means ± SEM of oxygen consumption (nmol O_2.min^{-1} mg^{-1} protein). Data were from at least four independent experiments. The residual oxygen consumption (ROX) was evaluated after 1.25 μg/mL AA addition. The respiratory control ratio (RCR) was calculated by dividing the uncoupled respiration by state 4-like respiratory rates.*, Student's *t*-test statistical analyses ($p<0.05$) for comparisons between trypomastigotes and epimastigotes

Increased complex II–III and reduced complex IV activities create an "electron bottleneck" in bloodstream trypomastigotes mitochondria

The lower oxygen consumption rates exhibited by trypomastigotes at the metabolic states associated with a higher electron flow (state 3 and uncoupled state) suggest that the observed functional changes are derived from the inhibition of the transport/oxidation machinery (substrate transport, tricarboxylic acid cycle, and the electron transport chain) and not the phosphorylation machinery (F_1F_o-ATP synthase, adenine nucleotide translocator, and phosphate carrier). Therefore, we assessed the activity of the mitochondrial complex II–III and complex IV of both parasite forms (Figs. 2a and b). Surprisingly, complex II–III activities were significantly higher in bloodstream trypomastigotes than in epimastigotes (Fig. 2a, $p<0.05$). However, cytochrome *c* oxidase activity was significantly higher in epimastigotes than in bloodstream trypomastigotes (Fig. 2b, $p<0.05$).

Citrate synthase activity is commonly employed to determine the content of functional mitochondria of different cells. Despite the kinetoplastids possessing only a single mitochondrion, we observed that citrate synthase activity significantly decreased in bloodstream trypomastigotes as compared to epimastigotes (Fig. 2c, $p<0.05$), suggesting that the mitochondrial functional content of both forms is different. A similar trend was also observed when measuring the functional content of the F_1F_o-ATP synthase, which was significantly lower in bloodstream trypomastigotes (Fig. 2d, $p<0.05$).

We quantified the expression levels of genes related to the ETC by quantitative PCR (Fig. 3). Consistent with enzymatic activity, the expression of succinate dehydrogenase (SDH) was significantly higher in bloodstream trypomastigotes ($p<0.001$). Also, trypomastigote mRNA levels of cytochrome *b* (a component of complex III) and subunit IV of cytochrome *c* oxidase (a component of complex IV) were significantly lower (Fig. 3).

Trypomastigotes at mitochondrial metabolic states with a high proton motive force produce more mitochondrial H_2O_2

We evaluated mitochondrial H_2O_2 release in digitonin-permeabilized parasites at different metabolic states (Table 3). In the absence of succinate, the rates of H_2O_2 release in trypomastigotes were significantly higher than those in epimastigotes (9.66±1.60 pmol H_2O_2.min^{-1} mg ptn^{-1} vs. 2.85±0.36 pmol H_2O_2.min^{-1} mg ptn^{-1}, respectively, $p<0.01$). A similar pattern was also observed when succinate was added to the permeabilized parasites, with rates of H_2O_2 formation in trypomastigotes being significantly higher than

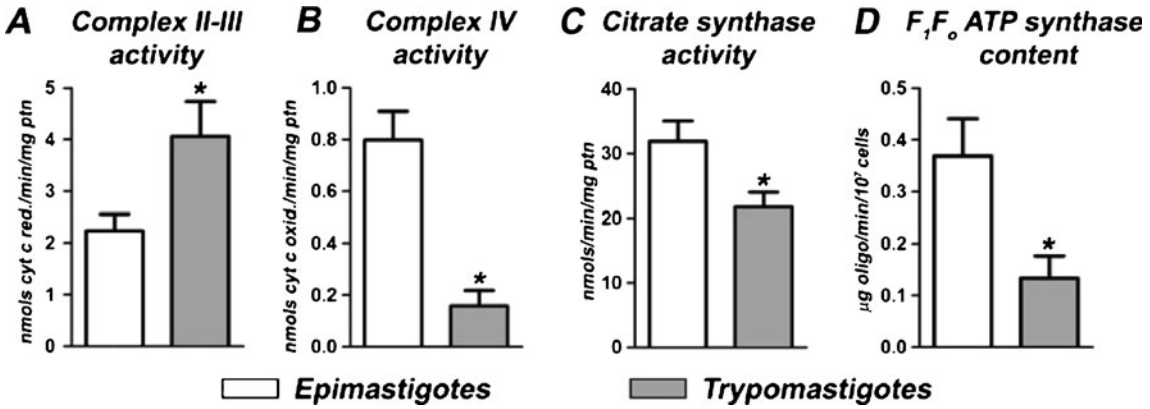

Fig. 2 Bloodstream trypomastigotes facilitate electron entry through the ETC but fail to allow electrons to exit through complex IV. (**a**) The activity of complex II–III was measured as the rate of antimycin A-sensitive ferricytochrome *c* reduction upon the addition of 5 mM succinate. (**b**) Complex IV activity was measured as the rate of KCN-sensitive ferrocytochrome *c* oxidation. (**c**) Citrate synthase activity was evaluated based on the rate of DTNB reduction. (**d**) F_1F_o ATP synthase functional content was measured by titrating the basal respiratory rates of parasites with oligomycin until complete inhibition of oxygen consumption rates was achieved. Epimastigotes were represented as white bars and bloodstream trypomastigotes as gray bars. * $p<0.05$, determined by the Student's *t*-test

in epimastigotes (24.54±3.78 pmol $H_2O_2.min^{-1}$ mg ptn^{-1} vs. 11.75±1.01 pmol $H_2O_2.min^{-1}$ mg ptn^{-1}, respectively, $p<0.01$). The addition of ADP did not affect mitochondrial H_2O_2 production in epimastigotes. Conversely, mitochondrial H_2O_2 production in trypomastigotes was significantly reduced by the addition of ADP (Table 3; 24.54±3.78 pmol $H_2O_2.min^{-1}$ mg ptn^{-1} (succinate) vs. 13.58±2.12 pmol $H_2O_2.min^{-1}$ mg ptn^{-1} (ADP), $p<0.05$). As expected, the impairment of F_1F_o-ATP synthase by oligomycin caused an increase in mitochondrial H_2O_2 production, which was more evident in bloodstream trypomastigotes than in epimastigotes

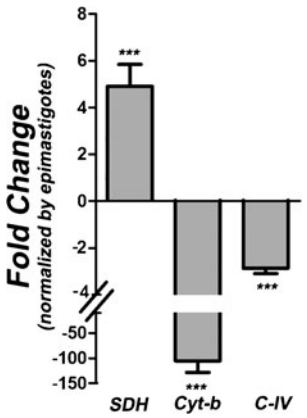

Fig. 3 Epimastigotes and bloodstream trypomastigotes differentially express ETC transcripts. The transcript levels of succinate dehydrogenase (Tc00.1047053505843.24), cytochrome *b* (Tc00.1047053509395.100) and cytochrome *c* oxidase, and subunit IV (Tc00.1047053510889.50) were evaluated in bloodstream trypomastigotes and normalized using the transcript levels of epimastigotes. Alpha-tubulin (Tc00.1047053411235.9) was used as an endogenous control. ***$p<0.0001$, comparison of transcript levels of each gene between epimastigotes and bloodstream trypomastigotes

(18.21±2.0 pmol $H_2O_2.min^{-1}$ mg ptn^{-1} vs. 13.6±0.99 pmol $H_2O_2.min^{-1}$ mg ptn^{-1}, respectively, $p<0.05$). The addition of FCCP collapsed the $\Delta\Psi_m$ and decreased H_2O_2 production in both parasite forms. Finally, the mitochondrial electron leak was quantified by dividing the rate of H_2O_2 production by the rate of oxygen consumption in each metabolic state of both forms (Herrero and Barja 1997). Figure 4 shows that the electron leak was significantly higher in trypomastigotes than in epimastigotes, regardless of the mitochondrial metabolic state. Interestingly, the increased electron leak upon the addition of succinate maybe due to increased activity in complex II–III in trypomastigotes (Fig. 2a), which is in agreement with recent evidence incriminating complex II as the main site of ROS production (Silva et al. 2011). These data demonstrate that mitochondrial H_2O_2 release in trypomastigotes is regulated by the $\Delta\Psi_m$ and is more efficient in metabolic states associated with a high proton motive force.

Table 3 H_2O_2 release in digitonin-permeabilized *T.* cruzi in the presence of FAD^+- linked substrate[a]

	Epimastigotes	Trypomastigotes
Mitochondrial metabolic states		
Parasite	2.85±0.36 (n=5)	9.66±1.6 (n=7)**
Succinate	11.75±1.01 (n=5)	24.54±3.78 (n=7)*
ADP	11.95±1.36 (n=6)	13.58±2.12 (n=7)
Oligo	13.6±0.99 (n=6)	18.21±2.0 (n=6)*
FCCP	11.13±1.42 (n=6)	10.17±1.69 (n=7)

[a] Values are expressed as means ± SEM of hydrogen peroxide generation npmol $H_2O_2.min^{-1}$ mg $protein^{-1}$). Data were from at least four independent experiments. * and ** Student's *t*-test statistical analyses, $p<0.05$ and $p<0.01$, respectively, for comparisons between trypomastigotes and epimastigotes

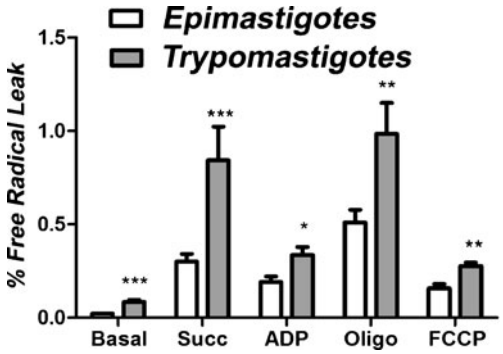

Fig. 4 Bloodstream trypomastigotes have increased electron leakage in comparison to epimastigotes. The free radical leak was considered as the percentage of total electron flow reducing oxygen to superoxide and ultimately hydrogen peroxide in the respiratory chain. The leak was measured as a ratio of mitochondrial H_2O_2 generated per O_2 consumed. The percentage of free radical leak in each mitochondrial metabolic state was evaluated in digitonin-permeabilized parasites after succinate addition. Student's *t*-tests were used to compare epimastigotes and trypomastigotes. * $p<0.05$; ** $p<0.001$; and *** $p<0.0001$

Discussion

The life cycle of *T. cruzi* was described more than 100 years ago (Chagas 1909), yet there is still no efficient treatment for Chagas' disease, despite the number of metabolic pathways that differ between the vertebrate host and the parasite. Because the bloodstream trypomastigotes are the circulating parasite stage inside the vertebrate host that is transmitted to the triatomine insect vector, it is crucial to understand the basic aspects of *T. cruzi* metabolism. In that sense, efforts to accomplish this goal have been hampered by difficulties in obtaining fresh bloodstream trypomastigotes in feasible amounts to perform biochemical and molecular investigations. Recently, a high throughput reverse genetics platform based on vector expression was generated (Batista et al. 2010) for use with *T. cruzi,* which lacks the necessary metabolic machinery to perform reverse genetics. For this reason, most recent data concerning trypanosomatid metabolism was obtained with *T. brucei*, for which genetic information that allows the knockdown of genes is available (Bringaud et al. 2006). Nevertheless, major differences were observed between *T. cruzi* and *T. brucei* metabolic pathways, especially regarding mitochondrial metabolism. Previous reports characterized the respiratory properties of *T. cruzi* epimastigotes (Affranchino et al. 1986; Vercesi et al. 1991) and the activities of select enzymes of the TCA cycle of epimastigotes (Adroher et al. 1988). Herein, we performed a functional assessment of the mitochondria of the following two distinct *T. cruzi* life forms: the vertebrate bloodstream trypomastigotes and the insect epimastigote forms. Our results indicate that mitochondrial metabolism of trypomastigotes facilitates electron entry and channeling in comparison with epimastigotes due to the increased activity of complex II–III and a downstream restriction in electron transport at complex IV, reducing oxygen consumption and allowing electron leak. These effects result in increased H_2O_2 generation. This mitochondrial functional plasticity in the *T. cruzi* life cycle may be paramount for adaptation, enabling parasites to survive in different hosts.

There is a steep variation in the availability of energy substrate among vertebrate blood, the intracellular environment, and the insect gut, and this variation imposes a great physiological challenge for the invading parasite. In the vertebrate bloodstream, trypomastigote forms have access to carbohydrates at a fairly constant concentration (5 mM glucose). Under such conditions, trypomastigotes opt to oxidize glucose rather than other carbon sources, such as free amino acids (Bringaud et al. 2006), and exhibit higher glucose transport activity in comparison to the other mammalian forms (Silber et al. 2009). A similar strategy is observed for bloodstream forms of *Trypanosoma brucei congolense* (Bienen et al. 1991). Bloodstream forms of *T. brucei* represent an extreme example of dependence on glycolysis because they lack both cytochromes and a classic respiratory chain (Tielens and Van Hellemond 1998). As soon as *T. cruzi* trypomastigotes reach the triatomine digestive tract, these parasites transform into epimastigote forms and metabolically adapt to the new environmental conditions. Apart from glucose, *T. cruzi* epimastigotes can utilize other carbon sources, such as free amino acids (Bringaud et al. 2006). In this regard, the triatomine midgut is glucose-poor but is rich in amino acids (Atwood et al. 2005; Bringaud et al. 2006; Silber et al. 2009) released from intense digestion of blood proteins, resulting in high hemolymphatic levels of histidine (Harington 1956; Harington 1961). Epimastigotes of *T. cruzi* are uniquely adapted to take advantage of this energy source by producing enzymes that can convert histidine to glutamate (Atwood et al. 2005), which is in turn converted to succinate, thereby providing reduced substrates for oxidative phosphorylation.

Our data demonstrate that bloodstream trypomastigotes are less dependent on the mitochondrial ETC (Table 1), which is consistent with previous observations that glucose uptake is higher in these parasite forms (Silber et al. 2009). Bloodstream trypomastigotes also exhibit reduced mitochondrial respiration (Table 2) and mitochondrial membrane potential ($\Delta\Psi_m$) (Fig. 1) in comparison with epimastigotes. Interestingly, proteomic analysis of *T. cruzi* evolutive forms revealed that there is a dramatic downregulation of glucose transporters and a simultaneous increase in the expression of enzymes involved in fatty acid oxidation during the transition from trypomastigote to intracellular amastigote forms. These data suggest a metabolic shift in response to this environmental change (Atwood et al. 2005).

Extracellular glucose levels regulate energy metabolism in different cells and organisms (Coustou et al. 2003; Lamour et al. 2005). Coustou and co-workers demonstrated that intracellular ATP levels of procyclic *T. brucei* grown in a glucose-rich medium are not altered by oligomycin, suggesting that oxidative phosphorylation is not fundamental for the survival of these parasite forms. In contrast, the downregulation of pyruvate kinase reduced ATP levels and increased the parasite doubling time (Coustou et al. 2003). Interestingly, procyclic forms of *T. brucei* kept in a medium mimicking the insect digestive tract containing limited glucose availability showed an increase in proline uptake and oligomycin sensitivity, suggesting that under limited availability of glucose, oxidative phosphorylation becomes the main source of ATP instead of glycolysis (Lamour et al. 2005). Similarly, *T. cruzi* bloodstream trypomastigotes were less sensitive to AA and were highly sensitive to IAA incubation (Table 1), indicating that these forms are less dependent on oxidative phosphorylation and rely more on glycolysis for ATP synthesis. These results were further supported by the reduced mitochondrial O_2 consumption and $\Delta\Psi_m$ of bloodstream trypomastigotes (Table 2 and Fig. 1).

In comparison with epimastigotes, metacyclic trypomastigotes of *T. cruzi* are better equipped with scavenger antioxidant defenses (Atwood et al. 2005; Piacenza et al. 2008), which can explain why they are more resistant to oxidative challenges despite their higher rates of mitochondrial H_2O_2 generation (Tables 1 and 3 and Fig. 5). Proteomic analyses have demonstrated an upregulation of several enzymes involved in antioxidant defenses in metacyclic trypomastigotes in comparison with epimastigotes, such as trypanothione synthetase, ascorbate peroxidase, mitochondrial and cytosolic tryparedoxin peroxidase, iron superoxide dismutase and tryparedoxin (Atwood et al. 2005; Piacenza et al. 2008). Differentiation from epimastigotes to metacyclic trypomastigotes was also correlated with increased resistance to peroxynitrite challenge (Piacenza et al. 2008). It is important to emphasize that the susceptibility of *T. cruzi* to H_2O_2 varies not only in any given individual parasite in the same strain, but also among different strains of the same parasite form (Boveris and Stoppani 1977; Mielniczki-Pereira et al. 2007). In addition, mitochondrial H_2O_2 generation varies among different strains of *T. cruzi* epimastigotes (Carranza

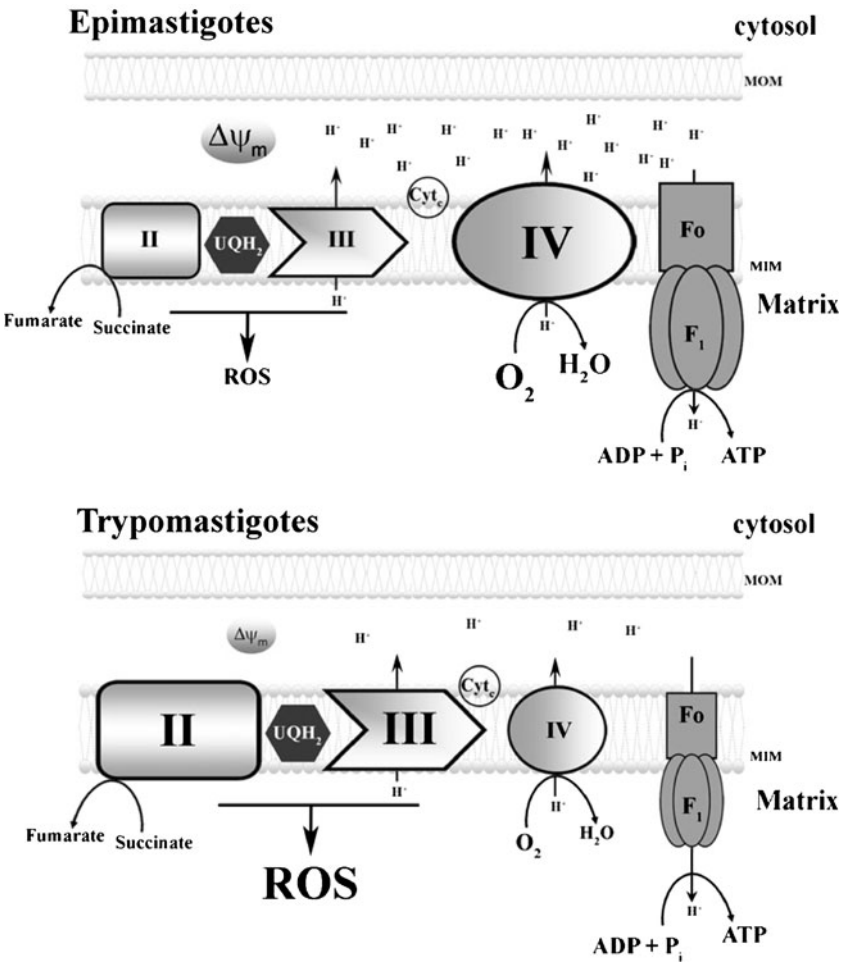

Fig. 5 Mitochondrial functional remodeling along *T. cruzi* life cycle. The main source of electrons for *T. cruzi* mitochondria was set to complex II by the addition of succinate. In this schematic representation, complex I was not represented as it has limited function in *T. cruzi* metabolism (Carranza et al. 2009). Bloodstream trypomastigotes exhibited increased complex II-III activities in comparison to epimastigotes (II, UQH_2, III). Conversely, complex IV (IV) activity in bloodstream forms was significantly reduced when compared to insect forms, creating an electron bottleneck that facilitates electron leakage and ROS formation. As a result, the $\Delta\Psi_m$ is reduced in bloodstream forms (represented as low amounts of H^+) as well as oxygen consumption. Further details are described in the text

et al. 2009). Our findings are consistent with the concept that bloodstream trypomastigotes are preadapted to oxidative challenges triggered by the host immune responses, such as the respiratory burst of phagocytic cells (Atwood et al. 2005). Nevertheless, additional research is required to determine which factors are involved in mitochondrial functional remodeling over the *T. cruzi* life cycle.

The mitochondrial functional changes observed in the two *T. cruzi* forms investigated in this study are schematically summarized in Fig. 5. In general, the mitochondria of both epimastigotes and bloodstream trypomastigotes operate in the classical way; oxidation of succinate supports not only the transference of electrons to oxygen, but also increases the membrane potential and supports H_2O_2 formation. However, striking differences were observed in the magnitude of all these parameters between the two parasite forms. Based on our data, we hypothesize that the reduced oxygen consumption and the increased electron leakage and H_2O_2 formation observed in bloodstream trypomastigotes could be a result of functional ETC remodeling. In bloodstream trypomastigotes, increased SDH expression and complex II–III activity facilitate the entry of electrons into the ETC (Figs. 2a and 3) while reducing cytochrome *b* and cytochrome *c* oxidase expression (Fig. 3) and activity (Fig. 2b). These alterations could restrict electron transport to the final site of ETC, resulting in an impairment of oxygen reduction to H_2O (Table 2), thereby creating an "electron bottleneck" effect. In this sense, higher electron leakage and H_2O_2 formation rates in bloodstream trypomastigotes could be a direct consequence of the restricted electron transport along the ETC (Fig. 5). Recent evidence indicates that mitochondrial-derived superoxide is an important molecule that drives preconditioning against stress conditions in yeast. In the same context, our data, in addition to previously reported data, show that trypomastigotes are more resistant to H_2O_2 and peroxynitrite incubation (Alvarez et al. 2011; Tanaka et al. 1983). A previous study also shows that bloodstream trypomastigotes are more equipped with antioxidant defenses (Irigoin et al. 2008). Additionally, more virulent parasite strains were more resistant to pro-oxidant injury and exhibited increased levels of antioxidant enzymes (Piacenza et al. 2009) compared to those in attenuated strains. Conceivably, increased mitochondrial ROS generation would precondition bloodstream trypomastigotes against a severe oxidative insult, in a hormetic-type response, protecting these parasite forms from the host immune response. Our results indicate that there is significant functional plasticity in the *T. cruzi* mitochondrion during different phases of its life cycle, which may be important for adaptation, enabling parasite survival in distinct host environments.

Acknowledgments This work was supported by grants from DECIT/SCTIE/MS, FIOCRUZ, FAPERJ and CNPq (through the Instituto Nacional de Ciência e Tecnologia em Biologia Estrutural e Bioimagem). MFO is a researcher scholar from CNPq and a recipient of the Jovens Cientistas do Nosso Estado grant from FAPERJ (2010). RLSG was funded by CAPES/FAPERJ. We are thankful for the technical support of Marcos Meuser and Michelle Fernandes. We are also grateful Dr. Jose Henrique M.C. Oliveira and Prof. Anibal E. Vercesi (Unicamp, Brazil) for the helpful discussions. Lastly, we thank Dr. Eduardo Fox for his assistance in manuscript revision.

References

Adroher FJ, Osuna A, Lupianez JA (1988) Differential energetic metabolism during *Trypanosoma cruzi* differentiation. I. Citrate synthase, NADP-isocitrate dehydrogenase, and succinate dehydrogenase. Arch Biochem Biophys 267(1):252–261

Affranchino JL, Schwarcz de Tarlovsky MN, Stoppani AO (1986) Terminal oxidases in the trypanosomatid *Trypanosoma cruzi*. Comp Biochem Physiol B 85(2):381–388

Alvarez MN, Peluffo G, Piacenza L, Radi R (2011) Intraphagosomal peroxynitrite as a macrophage-derived cytotoxin against internalized *Trypanosoma cruzi*: consequences for oxidative killing and role of microbial peroxiredoxins in infectivity. J Biol Chem 286(8):6627–6640

Atwood JA 3rd, Weatherly DB, Minning TA, Bundy B, Cavola C, Opperdoes FR et al (2005) The *Trypanosoma cruzi* proteome. Science 309(5733):473–476

Batista M, Marchini FK, Celedon PA, Fragoso SP, Probst CM, Preti H et al (2010) A high-throughput cloning system for reverse genetics in *Trypanosoma cruzi*. BMC Microbiol 10:259

Bienen EJ, Webster P, Fish WR (1991) *Trypanosoma (Nannomonas) congolense*: changes in respiratory metabolism during the life cycle. Exp Parasitol 73(4):403–412

Billingsley PF (1988) Morphometric analysis of *Rhodnius prolixus* Stal (Hemiptera:Reduviidae) midgut cells during blood digestion. Tissue & Cell 20(2):291–301

Boveris A, Chance B (1973) The mitochondrial generation of hydrogen peroxide. General properties and effect of hyperbaric oxygen. Biochemical Journal 134(3):707–716

Boveris A, Stoppani AO (1977) Hydrogen peroxide generation in *Trypanosoma cruzi*. Experientia 33(10):1306–1308

Bringaud F, Riviere L, Coustou V (2006) Energy metabolism of trypanosomatids: adaptation to available carbon sources. Mol Biochem Parasitol 149(1):1–9

Brookes PS, Levonen AL, Shiva S, Sarti P, Darley-Usmar VM (2002) Mitochondria: regulators of signal transduction by reactive oxygen and nitrogen species. Free Radic Biol Med 33(6):755–764

Carranza JC, Kowaltowski AJ, Mendonca MA, de Oliveira TC, Gadelha FR, Zingales B (2009) Mitochondrial bioenergetics and redox state are unaltered in *Trypanosoma cruzi* isolates with compromised mitochondrial complex I subunit genes. J Bioenerg Biomembr 41(3):299–308

Cazzulo JJ (1994) Intermediate metabolism in *Trypanosoma cruzi*. J Bioenerg Biomembr 26(2):157–165

Chagas, C. (1909). Nova tripanozomiaze humana: estudos sobre a morfolojia e o ciclo evolutivo do *Schizotrypanum cruzi* n. gen., n. sp., ajente etiolojico de nova entidade morbida do homem. Mem. Inst. Oswaldo Cruz, 1(2).

Chance B, Williams GR (1955) Respiratory enzymes in oxidative phosphorylation. II. Difference spectra. J Biol Chem 217(1):395–407

Chaudhuri M, Ott RD, Hill GC (2006) Trypanosome alternative oxidase: from molecule to function. Trends Parasitol 22(10):484–491

Coustou V, Besteiro S, Biran M, Diolez P, Bouchaud V, Voisin P et al (2003) ATP generation in the *Trypanosoma brucei* procyclic form: cytosolic substrate level is essential, but not oxidative phosphorylation. J Biol Chem 278(49):49625–49635

de Meirelles MN, De Souza W (1982) *Trypanosoma cruzi*: ultrastructural cytochemistry of mitochondrial enzymes. Exp Parasitol 53 (3):341–354

Denicola-Seoane A, Rubbo H, Prodanov E, Turrens JF (1992) Succinate-dependent metabolism in *Trypanosoma cruzi* epimastigotes. Mol Biochem Parasitol 54(1):43–50

Dias JC (2007) Globalization, inequity and Chagas disease. Cad Saude Publica 23(Suppl 1):S13–22

Docampo R (1993) Calcium homeostasis in *Trypanosoma cruzi*. Biol Res 26(1–2):189–196

Docampo R, Moreno SN, Vercesi AE (1993) Effect of thapsigargin on calcium homeostasis in *Trypanosoma cruzi* trypomastigotes and epimastigotes. Mol Biochem Parasitol 59(2):305–313

Ferguson M, Mockett RJ, Shen Y, Orr WC, Sohal RS (2005) Age-associated decline in mitochondrial respiration and electron transport in *Drosophila melanogaster*. Biochem J 390(Pt 2):501–511

Harington JS (1956) Histamine and histidine in excreta of the blood-sucking bug *Rhodnius prolixus*. Nature 178(4527):268

Harington JS (1961) Studies of the amino acids of *Rhodnius prolixus* I. Analysis of the haemolymph. Parasitology 51:309–318

Herrero A, Barja G (1997) ADP-regulation of mitochondrial free radical production is different with complex I-or complex II-linked substrates: implications for the exercise paradox and brain hypermetabolism. J Bioenerg Biomembr 29(3):241–249

Irigoin F, Cibils L, Comini MA, Wilkinson SR, Flohe L, Radi R (2008) Insights into the redox biology of *Trypanosoma cruzi*: Trypanothione metabolism and oxidant detoxification. Free Radic Biol Med 45(6):733–742

Japiassu AM, Santiago AP, d'Avila Jda C, Garcia-Souza LF, Galina A, Castro Faria-Neto HC et al (2011) Bioenergetic failure of human peripheral blood monocytes in patients with septic shock is mediated by reduced F1Fo adenosine-5′-triphosphate synthase activity. Crit Care Med 39(5):1056–1063

Korshunov SS, Skulachev VP, Starkov AA (1997) High protonic potential actuates a mechanism of production of reactive oxygen species in mitochondria. FEBS Lett 416(1):15–18

Kowaltowski AJ, de Souza-Pinto NC, Castilho RF, Vercesi AE (2009) Mitochondria and reactive oxygen species. Free Radic Biol Med 47(4):333–343

Lamour N, Riviere L, Coustou V, Coombs GH, Barrett MP, Bringaud F (2005) Proline metabolism in procyclic *Trypanosoma brucei* is down-regulated in the presence of glucose. J Biol Chem 280 (12):11902–11910

Lehane MJ (2005) The Biology of Blood-sucking in Insects, 2nd edn. Cambridge University, press, UK

Livak KJ, Schmittgen TD (2001) Analysis of relative gene expression data using real-time quantitative PCR and the 2(−Delta Delta C (T)) Method. Methods 25(4):402–408

Lowry OH, Rosebrough NJ, Farr AL, Randall RJ (1951) Protein measurement with the Folin phenol reagent. J Biol Chem 193 (1):265–275

Menna-Barreto RF, Goncalves RL, Costa EM, Silva RS, Pinto AV, Oliveira MF et al (2009) The effects on *Trypanosoma cruzi* of novel synthetic naphthoquinones are mediated by mitochondrial dysfunction. Free Radic Biol Med 47(5):644–653

Michels PA, Bringaud F, Herman M, Hannaert V (2006) Metabolic functions of glycosomes in trypanosomatids. Biochim Biophys Acta 1763(12):1463–1477

Mielniczki-Pereira AA, Chiavegatto CM, Lopez JA, Colli W, Alves MJ, Gadelha FR (2007) *Trypanosoma cruzi* strains, Tulahuen 2 and Y, besides the difference in resistance to oxidative stress, display differential glucose-6-phosphate and 6-phosphogluconate dehydrogenases activities. Acta Trop 101(1):54–60

Nicholls DG, Ferguson SJ (2002) Bioenergetics 3, 3rd edn. London, Academic Press, pp 82–83

Pan Y, Schroeder EA, Ocampo A, Barrientos A, Shadel GS (2011) Regulation of Yeast Chronological Life Span by TORC1 via Adaptive Mitochondrial ROS Signaling. Cell Metab 13(6):668–678

Piacenza L, Peluffo G, Alvarez MN, Kelly JM, Wilkinson SR, Radi R (2008) Peroxiredoxins play a major role in protecting *Trypanosoma cruzi* against macrophage-and endogenously-derived peroxynitrite. Biochem J 410(2):359–368

Piacenza L, Zago MP, Peluffo G, Alvarez MN, Basombrio MA, Radi R (2009) Enzymes of the antioxidant network as novel determiners of *Trypanosoma cruzi* virulence. Int J Parasitol 39 (13):1455–1464

Poyton RO, McEwen JE (1996) Crosstalk between nuclear and mitochondrial genomes. Annu Rev Biochem 65:563–607

Rogerson GW, Gutteridge WE (1980) Catabolic metabolism in *Trypanosoma cruzi*. Int J Parasitol 10(1):131–135

Rozen S, Skaletsky H (2000) Primer3 on the WWW for general users and for biologist programmers. Methods Mol Biol 132:365–386

Silber AM, Tonelli RR, Lopes CG, Cunha-e-Silva N, Torrecilhas AC, Schumacher RI et al (2009) Glucose uptake in the mammalian stages of *Trypanosoma cruzi*. Mol Biochem Parasitol 168 (1):102–108

Silva TM, Peloso EF, Vitor SC, Ribeiro LH, & Gadelha FR (2011). O (2) consumption rates along the growth curve: new insights into *Trypanosoma cruzi* mitochondrial respiratory chain. J Bioenerg Biomembr. [ahead of print]

Tanaka Y, Tanowitz H, Bloom BR (1983) Growth of *Trypanosoma cruzi* in a cloned macrophage cell line and in a variant defective in oxygen metabolism. Infect Immun 41(3):1322–1331

Tanowitz HB, Weiss LM, Montgomery SP (2011) Chagas disease has now gone global. PLoS Negl Trop Dis 5(4):e1136

Tielens AG, Van Hellemond JJ (1998) Differences in energy metabolism between trypanosomatidae. Parasitol Today 14 (7):265–272

Tielens AG, van Hellemond JJ (2009) Surprising variety in energy metabolism within Trypanosomatidae. Trends Parasitol 25 (10):482–490

Vercesi AE, Bernardes CF, Hoffmann ME, Gadelha FR, Docampo R (1991) Digitonin permeabilization does not affect mitochondrial function and allows the determination of the mitochondrial membrane potential of *Trypanosoma cruzi* in situ. J Biol Chem 266(22):14431–14434

Villani G, Attardi G (2000) In vivo control of respiration by cytochrome c oxidase in human cells. Free Radic Biol Med 29 (3–4):202–210

Villani G, Greco M, Papa S, Attardi G (1998) Low reserve of cytochrome c oxidase capacity in vivo in the respiratory chain of a variety of human cell types. J Biol Chem 273(48):31829–31836

Votyakova TV, Reynolds IJ (2004) Detection of hydrogen peroxide with Amplex Red: interference by NADH and reduced glutathione auto-oxidation. Arch Biochem Biophys 431(1):138–144

Zuckerbraun BS, Chin BY, Bilban M, d'Avila JC, Rao J, Billiar TR et al (2007) Carbon monoxide signals via inhibition of cytochrome c oxidase and generation of mitochondrial reactive oxygen species. FASEB J 21(4):1099–1106